

Formation of SiO₂ Air-Gap Patterns Through scCO₂ Infusion of NIL Patterned PHEMA

John R. Ell,[†] Todd A. Crosby,[‡] Joseph J. Peterson,[†] Kenneth R. Carter,^{*,†} and James J. Watkins^{*,†}

[†]Polymer Science and Engineering Department, University of Massachusetts—Amherst, Conte Center for Polymer Research, 120 Governors Drive, Amherst, Massachusetts 01003 and [‡]Chemical Engineering Department, University of Massachusetts—Amherst, 159 Goessman Lab, Amherst, Massachusetts 01003

Received July 29, 2009. Revised Manuscript Received November 23, 2009

Using templates generated by nanoimprint lithography, we report the fabrication of SiO₂ patterns (~450 nm) line widths over large active surface areas (14.5 cm²). The process involves the patterning of poly(2-hydroxyethyl methacrylate) (PHEMA) using polycarbonate molds followed by tetrachlorosilane (TCS) vapor cross-linking and supercritical carbon dioxide (scCO₂) assisted tetraethylorthosilicate (TEOS) infusion. Uniform SiO₂ lines were observed over an area 14.5 cm², which suggests that this process can be readily scaled.

Introduction

Standard methods for the generation of silicon dioxide (SiO₂) patterns onto thermal and native oxide thin-film substrates such as etching through a photolithographic resist, beam lithography,¹ laser ablation,² polymer template etch masking,^{3–5} and holographic lithography⁶ are typically time intensive and involve subtractive processing schemes. Although these techniques can provide extreme precision over multiple length scales (25–500 nm), they are generally not well-suited to high throughput processing and often lack economic viability for the commercial production of low cost devices including optical waveguides,² diffraction gratings,^{7,8} and microfluidics.⁹ Over the past few years, a number of novel, cost-effective,

and high-throughput patterning techniques such as step and flash imprint lithography (SFIL),¹⁰ micro molding in capillaries (MIMIC),^{11,12} high-efficiency stepwise contraction adsorption nanolithography (h-SCAN),¹³ and easy soft imprint nanolithography (ESNIL)¹⁴ have been reported for precise replication of microscale and nanoscale patterns over large active surface areas. A large number of these patterning techniques use poly(dimethylsiloxane) (PDMS) molds created from Si masters. Most recently, precise control of these patterned dimensions was demonstrated by the mechanical stretching of a PDMS mold through a small stepwise manipulation process to imprint an absorbed solution of propyltrimethoxysilane onto a glass substrate.¹² The subsequent patterned features were fixed to the glass substrate following condensation of the silanol groups to create lines of SiO₂. However, these PDMS molds were generated from masters consisting of commercial diffraction gratings.

Implementation of high-throughput nanopatterning in most cases will require high precision master molds with active surface areas ranging from 1 to 2.5 cm². A number of materials have been examined for use in molds ranging from hard inorganic materials (oxides, silicon, metals, etc.) to “soft” materials including numerous polymers. Inorganic molds are usually fabricated by costly, time intensive photolithographic processes such as electron beam (e-beam) or deep UV lithography. For this reason, the use of daughter molds has become an attractive

*Corresponding author. E-mail: krcarter@polysci.umass.edu (K.R.C.); watkins@polysci.umass.edu (J.J.W.).

- (1) Della Giustina, G.; Guglielmi, M.; Brusatin, G.; Prasciolu, M.; Romanato, F. *J. Sol–Gel Sci. Technol.* **2008**, *48*(1), 212–216.
- (2) Flores-Arias, M. T.; Castelo, A.; Gomez-Reino, C.; de la Fuente, G. F. *Opt. Commun.* **2009**, *282*(6), 1175–1178.
- (3) Aissou, K.; Kogelschatz, M.; Baron, T.; Gentile, P. *Surf. Sci.* **2007**, *601*(13), 2611–2614.
- (4) Pai, R. A.; Humayun, R.; Schulberg, M. T.; Sengupta, A.; Sun, J. N.; Watkins, J. J. *Science* **2004**, *303*, 507.
- (5) Yin, D.; Horiuchi, S.; Masuoka, T. *Chem. Mater.* **2005**, *17*(3), 463–469.
- (6) Carvalho, E. J.; Alves, M. A. R.; Braga, E. S.; Cescato, L. *Microelectron. J.* **2006**, *37*(11), 1265–1270.
- (7) Chu, J. P.; Wijaya, H.; Wu, C. W.; Tsai, T. R.; Wei, C. S.; Nieh, T. G.; Wadsworth, J. *Appl. Phys. Lett.* **2007**, *90*(3), 034101–3.
- (8) Shih, T.-K.; Ho, J.-R.; Liao, H.-Y.; Chen, C.-F.; Liu, C.-Y. *Thin Solid Films* **2008**, *516*(16), 5339–5343.
- (9) Mizoshiri, M.; Nishiyama, H.; Nishii, J.; Hirata, Y. SiO₂-based variable microfluidic lenses fabricated by femtosecond laser lithography-assisted micromachining. In *Nanoengineering: Fabrication, Properties, Optics, and Devices V*; San Diego, CA: SPIE: Bellingham, WA, 2008; Vol. 7039, pp 70390E–70390E8.
- (10) Bailey, T.; Choi, B. J.; Colburn, M.; Meissl, M.; Shaya, S.; Ekerdt, J. G.; Sreenivasan, S. V.; Willson, C. G. Step and flash imprint lithography: Template surface treatment and defect analysis. *Papers from the 44th International Conference on Electron, Ion, And Photon Beam Technology and Nanofabrication*; Rancho Mirage, CA, 2000; American Vacuum Society: New York, 2000; pp 3572–3577.

- (11) Kim, E.; Xia, Y.; Whitesides, G. M. *Nature* **1995**, *376*(6541), 581–584.
- (12) Benahmed, A.; Lam, R.; Rechner, N.; Ho, C.-M. *J. Micro/Nanolithogr., MEMS, MOEMS* **2007**, *6*(2), 023007–5.
- (13) Tan, L.; Ouyang, Z.; Liu, M.; Ell, J.; Hu, J.; Patten, T. E.; Liu, G.-y. *J. Phys. Chem. B* **2006**, *110*(46), 23315–23320.
- (14) Moran, I. W.; Briseno, A. L.; Loser, S.; Carter, K. R. *Chem. Mater.* **2008**, *20*(14), 4595–4601.

alternative wherein a single master can be used to create multiple NIL daughter molds. A recent review highlights many of these applications.¹⁵

A great many soft materials have been successfully utilized as molds in NIL. Examples include siloxanes,^{16–18} cured UV photopolymers,^{19–21} fluoropolymers,^{22,23} poly vinyl alcohol,²⁴ polystyrene,²⁵ thiol-enes,²⁶ and polycarbonate.²⁷ In each case, the thermal, optical, and mechanical properties of the polymer has to be carefully matched to the specific NIL process. Additionally, emerging research in nanobiology and chemistry has applied pressure to fluidic device fabrication to reach nanoscale features.^{28–30} Improving the sensitivity of devices for biosensing,³¹ size exclusion chromatography for small molecule and nanoparticle separation,³² fluid transport,³³ and the fundamental study of molecular behavior³⁴ has reached fundamental challenges with the limited availability of low-cost functional nanofluidic devices.^{11,35–37} For example, arrays of regularly spaced micrometer scale pillars have been used to separate long DNA molecules with some success but have not reached the efficiency of pulsed field gel electrophoresis.³⁸ It is predicted that nanometer scaled devices will aid in this endeavor.

The biocompatible and nontoxic nature of poly(hydroxyethylmethacrylate) (HEMA) has made it an attractive choice for biomedical applications such as soft contact lens materials,³⁹ bone implants,⁴⁰ and controlled drug release.⁴¹ PHEMA has recently found use as a readily removable lift-off layer for lithographic patterning as well as a template for selective photolithographic cross-linking in the presence of a photo acid generator (PAG) and the acid sensitive cross-linking agent tetrakis-(methoxymethyl) glycouracil (TMMGU).^{14,42,43} Here, we report the first demonstration of the use of polycarbonate molds to perform NIL into PHEMA. We then infuse and selectively deposit SiO₂ within imprinted PHEMA layers to produce high-fidelity air-gap SiO₂ replicas following calcination of the mold.

Silica deposition can be performed using a variety of techniques such as plasma enhanced chemical vapor deposition (PECVD),⁴⁴ liquid phase deposition (LDP),^{45,46} e-beam evaporation (EBE),⁴⁶ and atomic layer deposition (ALD).⁴⁷ Each technique exhibits its own limitations, such as nonconformal coating, invasive deposition conditions, time-consuming fabrication, and low concentrations of precursors, respectively. A new approach to directly pattern mesoporous SiO₂ materials through photolithography of block copolymer templates followed by scCO₂-mediated selective silica condensation has recently been demonstrated.^{48,49} One advantage of the process is that subsequent etching is not required such that subtractive processing is eliminated. The polymer templates were either BASF Pluronic (amphiphilic triblock copolymers) or diblock copolymers that can be deprotected in the same manner as chemically amplified photoresists to yield patterned amphiphilic templates. In both cases, the templates are loaded with a photoacid generator that, upon exposure, yields strong acids in the exposed regions to selectively catalyze SiO₂ condensation. This process has been demonstrated with various metal alkoxides in scCO₂ with selective infusion of the inorganic materials into the hydrophilic block copolymer domains to yield patterned thin films with ordered mesoporousity.^{49–52} The

- (15) Schift, H. *J. Vac. Sci. Technol., B* **2008**, 26(2), 458–480.
- (16) Choi, W. M.; Park, O. O. *Microelectron. Eng.* **2004**, 73–74, 178–183.
- (17) Bender, M.; Plachetka, U.; Ran, J.; Fuchs, A.; Vratzov, B.; Kurz, H.; Glinsner, T.; Lindner, F. *J. Vac. Sci. Technol., B* **2004**, 22(6), 3229–3232.
- (18) Odom, T. W.; Love, J. C.; Wolfe, D. B.; Paul, K. E.; Whitesides, G. M. *Langmuir* **2002**, 18(13), 5314–5320.
- (19) Kim, Y. S.; Lee, N. Y.; Lim, J. R.; Lee, M. J.; Park, S. *Chem. Mater.* **2005**, 17(23), 5867–5870.
- (20) McClelland, G. M.; Hart, M. W.; Rettner, C. T.; Best, M. E.; Carter, K. R.; Terris, B. D. *Appl. Phys. Lett.* **2002**, 81(8), 1483–1485.
- (21) von Werne, T. A.; Germack, D. S.; Hagberg, E. C.; Sheares, V. V.; Hawker, C. J.; Carter, K. R. *J. Am. Chem. Soc.* **2003**, 125(13), 3831–3838.
- (22) Khang, D. Y.; Lee, H. H. *Langmuir* **2004**, 20(6), 2445–2448.
- (23) Rolland, J. P.; Hagberg, E. C.; Denison, G. M.; Carter, K. R.; De Simone, J. M. *Angew. Chem., Int. Ed.* **2004**, 43(43), 5796–5799.
- (24) Schaper, C. D.; Miahnahri, A. Polyvinyl alcohol templates for low cost, high resolution, complex printing. *48th International Conference on Electron, Ion, and Photon Beam Technology and Nanofabrication*; San Diego, CA, Jun 1–4, 2004; American Vacuum Society: New York, 2004; pp 3323–3326.
- (25) Harrer, S.; Strobel, S.; Scarpa, G.; Abstreiter, G.; Tornow, M.; Lugli, P. *IEEE Trans. Nanotechnol.* **2008**, 7(3), 363–370.
- (26) Hagberg, E. C.; Malkoch, M.; Ling, Y. B.; Hawker, C. J.; Carter, K. R. *Nano Lett.* **2007**, 7(2), 233–237.
- (27) Pisignano, D.; D'Amone, S.; Gigli, G.; Cingolani, R. *J. Vac. Sci. Technol., B* **2004**, 22(4), 1759–1763.
- (28) Zhang, B.; Wood, M.; Lee, H. *Anal. Chem.* **2009**, 81(13), 5541–5548.
- (29) Thorsen, T.; Maerkl, S. J.; Quake, S. R. *Science* **2002**, 298(5593), 580–584.
- (30) Craighead, H. G. *Science* **2000**, 290(5496), 1532–1535.
- (31) Li, J.; Gershow, M.; Stein, D.; Brandin, E.; Golovchenko, J. A. *Nat. Mater.* **2003**, 2(9), 611–615.
- (32) Storm, A. J.; Chen, J. H.; Ling, X. S.; Zandbergen, H. W.; Dekker, C. *Nat. Mater.* **2003**, 2(8), 537–540.
- (33) Turner, S. W. P.; Cabodi, M.; Craighead, H. G. *Phys. Rev. Lett.* **2002**, 88(12), 128103.
- (34) Levene, M. J.; Koriach, J.; Turner, S. W.; Foquet, M.; Craighead, H. G.; Webb, W. W. *Science* **2003**, 299(5607), 682–686.
- (35) Enoch, K.; Younan, X.; George, M. W. *Adv. Mater.* **1996**, 8(3), 245–247.
- (36) Yang, P. D.; Deng, T.; Zhao, D. Y.; Feng, P. Y.; Pine, D.; Chmelka, B. F.; Whitesides, G. M.; Stucky, G. D. *Science* **1998**, 282, 2244.
- (37) Yang, P.; Rizvi, A. H.; Messer, B.; Chmelka, B. F.; Whitesides, G. M.; Stucky, G. D. *Adv. Mater.* **2001**, 13(6), 427–431.
- (38) Eijkel, J. C. T.; Berg van den, A. *Microfluid. Nanofluid.* **2005**, 1(3), 249–267.

- (39) Barrett, G. D.; Constable, I. J.; Stewart, A. D. *J. Cataract Refract. Surg.* **1986**, 12(6), 623–31.
- (40) Hutcheon, G. A.; Messiou, C.; Wyre, R. M.; Davies, M. C.; Downes, S. *Biomaterials* **2001**, 22(7), 667–676.
- (41) Robert, C. C. R.; Buri, P. A.; Peppas, N. A. *J. Controlled Release* **1987**, 5(2), 151–7.
- (42) Moran, I. W.; Cheng, D. F.; Jhaveri, S. B.; Carter, K. R. *Soft Matter* **2008**, 4(1), 168–176.
- (43) Ford, J.; Yang, S. *Chem. Mater.* **2007**, 19(23), 5570–5575.
- (44) Wickramanayaka, S.; Nakanishi, Y.; Hatanaka, Y. *Appl. Surf. Sci.* **1997**, 113–114, 670–674.
- (45) Chou, J.-S.; Lee, S.-C. *Appl. Phys. Lett.* **1994**, 64(15), 1971–1973.
- (46) Jiun-Lin, Y.; Si-Chen, L. *IEEE Electron Device Lett.* **1999**, 20(3), 138–139.
- (47) Cameron, M. A.; Gartland, I. P.; Smith, J. A.; Diaz, S. F.; George, S. M. *Langmuir* **2000**, 16(19), 7435–7444.
- (48) Nagarajan, S.; Bosworth, J. K.; Ober, C. K.; Russell, T. P.; Watkins, J. J. *Chem. Mater.* **2008**, 20(3), 604–606.
- (49) Pai, R. A.; Humayun, R.; Schulberg, M. T.; Sengupta, A.; Sun, J.-N.; Watkins, J. J. *Science* **2004**, 303(5657), 507–510.
- (50) Tirumala, V. R.; Pai, R. A.; Agarwal, S.; Testa, J. J.; Bhatnagar, G.; Romang, A. H.; Chandler, C.; Gorman, B. P.; Jones, R. L.; Lin, E. K.; Watkins, J. J. *Chem. Mater.* **2007**, 19(24), 5868–5874.
- (51) Pai, R. A.; J. J. W. *Adv. Mater.* **2006**, 18(2), 241–245.
- (52) Chen, H.-T.; Crosby, T. A.; Park, M.-H.; Nagarajan, S.; Rotello, V. M.; Watkins, J. J. *J. Mater. Chem.* **2009**, 19(1), 70–74.

advantage of this approach is that there exists a separation between the preparation of the ordered polymer template and the inorganic network formation. This enables manipulation of the template prior to the formation of the metal oxide. It was shown that the scCO_2 slightly dilates the polymer template and does not interfere with the well-ordered structure.⁵³

Herein, a robust process for creating patterned SiO_2 air-gap structures using polycarbonate molds by selectively infusing a PHEMA polymer template through scCO_2 mediated silica condensation is demonstrated. This technique was utilized to form uniform submicrometer air-gap patterns of SiO_2 over large surface areas in order to limit the cost and time involved in accessing Si master molds.

Experimental Section

Materials. Tetraethylorthosilicate (99%) and 2-hydroxyethyl methacrylate (98%) were purchased from Acros Organics. Tetrachlorosilane (98%) was purchased from Gelest. Ethanol and methanol (anhydrous) were purchased from Fisher Scientific. Silicon substrates Sumco Phenix (1–0–0), type P, Boron doped, 5–80 resistivity, and a thickness of 700–750 μm were purchased from WaferNet Inc. Polycarbonate molds were created using Verbatim DataLifePlus inkjet printable DVD-R media purchased from commercial sources. All other reagents were purchased from Sigma-Aldrich and used without further purification. All reactions were run under N_2 unless otherwise noted. I-CHEM series 200 short clear WM septa jars (125 mL) were used for vapor cross-linking of the PHEMA films.

Instrumentation. Glass-transition temperatures (T_g) were determined using a TA Instruments Q2000 differential scanning calorimeter (DSC) using a heat/cool/heat run cycle at 10 $^\circ\text{C}/\text{min}$. Thermogravimetric analysis (TGA) was performed in nitrogen atmosphere on a DuPont TGA 2950 using a ramp rate of 10 $^\circ\text{C}/\text{min}$ under N_2 . Film thicknesses were measured using a Veeco Dektak 150 profilometer. The water contact angles were measured using a VCA Optima surface analysis/goniometry system with a drop size of 0.5 μL . Atomic force microscopy (AFM) images were collected on a Digital Instruments Nanoscope III in tapping mode under ambient conditions using silicon cantilevers (spring constant 0.58 N/m). RMS roughness and feature dimensions were calculated with the AFM manufacturer's provided software on 5 $\mu\text{m} \times 5 \mu\text{m}$ scan size images. Statistical analysis was also performed on each image using full width at half-maximum. Attenuated total reflection fourier transform infrared spectroscopy (ATR-FTIR) spectra were recorded under a constant N_2 stream using a Nicolet 6700 FT-IR spectrometer equipped with a Harrick grazing angle ATR accessory (GATR) and a liquid-nitrogen-cooled photovoltaic detector (LN-MCT). Spectra were recorded under a steady flow of N_2 to minimize absorbance peaks due to moisture and CO_2 at 128 scans with a 4 cm^{-1} resolution. A Phantom III ICP reactive ion etcher (RIE) from Trion Technology Inc. was used for oxygen plasma cleaning of each substrate. Each wafer was cut into (3.8 $\text{cm} \times 3.8 \text{ cm}$) pieces then washed with hexane, acetone, and isopropyl alcohol followed by an O_2 plasma cleaning procedure at a flow rate of 49 standard cubic centimeters per minute (sccm), with the inductive coupled

plasma (ICP) power at 500 W and the reactive ion etching (RIE) power at 200 W for 300 s. Gel-permeation chromatography (GPC) was performed on a Polymer Laboratories PL-GPC 50 with DMF and calibrated with PMMA standards. Imprinting into PHEMA was performed on a Nanonex NX2000 thermal imprinter. Sample preparation by focus ion beam (FIB) was performed using an FEI Nova 600 Nanolab dual beam FIB which was also used for collection of cross-sectional SEM images. The procedure involves the deposition of $\sim 400 \text{ nm}$ of platinum as a protection layer followed by FIB etching through $\sim 2 \mu\text{m}$. In Figure 4B, the mound above the patterned lines is the platinum. The images were performed at 52.3 $^\circ$ angle to get the cross-sectional image.

Synthesis of Poly(2-hydroxymethyl methacrylate) PHEMA. Ethanol (7.5 mL) was added to a test tube and nitrogen was bubbled through it for 5 min. AIBN (0.07 g, 0.43 mmol), HEMA (5.37 g, 5 mL, and 41.31 mmol), and dodecane thiol (0.43 g, 0.5 mL) were added and the solution was heated under N_2 at 60 $^\circ\text{C}$ for 4 h. The solution was then cooled down and the product precipitated dropwise in ethyl ether. The polymer was filtered, washed excessively with ethyl ether, and dried in vacuo at 50 $^\circ\text{C}$ for 48 h to yield a fine white powder (4.5 g, 83%), $M_n = 8.7 \text{ k g/mol}$, $\text{PDI} = 1.9$ (DMF vs PMMA) ($T_g = 73.49 \text{ }^\circ\text{C}$).⁴²

Preparation of Polycarbonate Master Mold. The polycarbonate mold was prepared from a commercially available DVD-R disk that was split into two pieces by carefully separating the two polycarbonate discs in the center ring with a spatula. The separation process results in two polycarbonate discs one with a metal coating and the other coated with a purple organic dye. The disk coated with the organic dye was washed with ethanol and dried under a stream of N_2 to prevent fouling of the mold with the organic dye. Uniform trapezoidal pieces (5 $\text{cm} \times 5 \text{ cm}$) were cut from the disk and the embossed edges at each of the bases of the trapezoid were removed. No chemical modification of the polycarbonate mold was needed. The measurement of the mold dimensions was performed through the replication of the polycarbonate disk into Sylgard 184 cured at 60 $^\circ\text{C}$ for 24 h.

Patterning via Nanoimprint Lithography (NIL). A 3 wt % (solids/total solution) solution of PHEMA containing 0.1 wt % poly(ethylene glycol) monomethylether (PEO, $M_n = 2000 \text{ g/mol}$) and 0.2 wt % *p*-toluene sulfonic acid monohydrate (pTSA) in ethanol (filtered through 0.45 μm PTFE syringe filter) was spin-coated onto a (3.8 $\text{cm} \times 3.8 \text{ cm}$) silicon substrate at 3000 rpm for 20 s. The resulting thin films (105 nm) were patterned with a freshly cleaned polycarbonate mold using a NX2000 thermal imprinter with the following conditions: the preprint was made at 50 $^\circ\text{C}$ at 0.69 MPa (100 psi) for 30 s, printed at 90 $^\circ\text{C}$ at 1.72 MPa (250 psi) for 30 s, and cooled to 38 $^\circ\text{C}$, and then the pressure was released. The printing procedure resulted in near-perfect replication of the polycarbonate mold into the PHEMA thin film with minimal observed defects.

Cross-Linking of PHEMA Films. The general procedure for vapor infusing and cross-linking the PHEMA films with tetrachlorosilane (TCS) was as follows. The patterned PHEMA wafers were placed on a glass pedestal in a I-CHEM jar (60 mL) with a PTFE screw top and vacuum/backfilled three times with N_2 followed by a 20 min N_2 purge. Tetrachlorosilane (50 μL) was injected on the bottom of the jar then sealed with Parafilm and left at room temperature for 12 h. The patterned wafer was then removed and analyzed.

Supercritical Carbon Dioxide Silica Mediated Infusion of Patterned PHEMA Films. The TCS cross-linked patterned PHEMA films were replicated in silica via supercritical carbon dioxide (scCO_2) mediated silica condensation. After lightly

(53) Gupta, R. R.; Ramachandra Rao, V. S.; Watkins, J. J. *Macromolecules* **2003**, 36(4), 1295–1303.

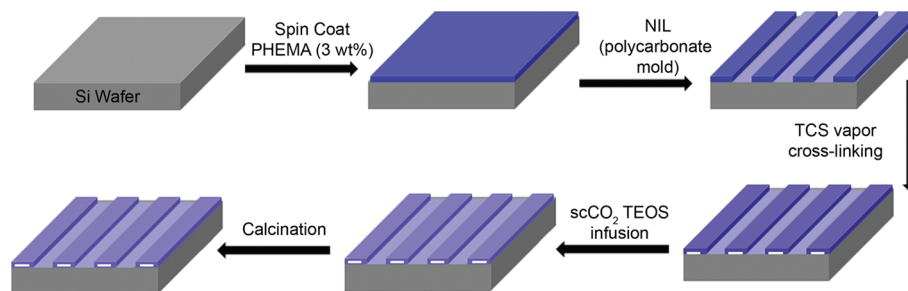


Figure 1. Schematic of direct SiO₂ infusion of patterned PHEMA thin-films.

cross-linking, the substrate was placed in a 140 mL stainless steel high-pressure reactor at room temperature with 25–50 μL of water and approximately 5 μL of tetraethylorthosilicate (TEOS) per cm^2 of patterned substrate. Approximately 35 mL of carbon dioxide (Merriam-Graves Coleman grade) at 69 bar and room temperature was injected into the sealed reactor via a syringe pump within 20 min. Immediately after injection, the wall temperature was heated to 220 $^{\circ}\text{C}$, which brought the gas to a temperature of 160 $^{\circ}\text{C}$ over 2 h while increasing the pressure to 120 bar. The system was allowed to react at the elevated pressure and temperature for at least 12 h then depressurized over 20 min. These conditions were optimized from literature procedures.^{54,55} The organic PHEMA template was removed via high-temperature calcination at 400 $^{\circ}\text{C}$ for 6 h with a ramp rate of 1.67 $^{\circ}\text{C}/\text{min}$.

Results and Discussion

The different steps of the direct SiO₂ infusion of patterned PHEMA films are illustrated in Figure 1. First, uniform PHEMA thin films (~ 105 nm) were prepared by spin-coating a 3 wt % solution of PHEMA, poly(ethylene oxide) (PEO), and pTSA onto a freshly cleaned (O₂ plasma etched) Si wafer (3.8 cm \times 3.8 cm). Process conditions were optimized in order to minimize the thickness of the residual scum layer, which will allow this process to easily be extrapolated to patterns that consist of isolated free-standing features. The addition of PEO as a plasticizing agent improved the quality of the imprint and was observed to be essential for imprinting films (< 100 nm) with smaller feature height molds, an effect that will be discussed in greater detail in a forthcoming publication. Previously published reports in our group used Pluronics and diblock copolymer templates to generate patterned mesoporous silicon dioxide materials through photolithography paired with supercritical carbon dioxide (scCO₂) mediated infusion.^{48,49} It was reported that the tetraethylorthosilicate (TEOS) infusion required the addition of pTSA in order to facilitate acid catalyzed silica condensation. The addition of pTSA was also determined to be necessary in our PHEMA polymer template for selective silica infusion.

The inherent hydroxyl chemical functionality of PHEMA was utilized by the postfunctionalization of the patterns through TEOS infusion. The PHEMA hydrophilicity presented both positive and negative attributes to the processing of the patterned substrates. The hydrophilicity of the PHEMA thin film helped simplify the NIL

printing procedure by allowing the use for polycarbonate molds without any further modification. On the other hand, sample preparation required great care in preventing adsorption of ambient water, which competitively reacts with chlorosilanes used as the cross-linking agent in the next step. The adsorption of water was limited by storing each sample directly after imprinting in a desiccator.

Polycarbonate molds were made from commercially available DVD-R media, due to their low cost and ready availability. Optical disk media (CD's, DVD's, HD-DVD's, and Blu-Ray discs (~ 220 nm, ~ 1.2 μm), (~ 190 nm, ~ 500 nm), (~ 70 nm, ~ 240 nm), and (~ 20 nm, ~ 180 nm) (height, line width), respectively) that consist of patterned polycarbonate sandwiched between reflective layers contain features of technologically useful size, pitch, and aspect ratio, making them ideal for exploring new NIL processes. These discs have been utilized in micro- and nanopatterning of spin-transition compounds,⁵⁶ micro-transfer molding (μTM),⁵⁷ and roll-to-roll processing.⁵⁸ The polycarbonate master mold was prepared by first separating the laminated layers of a polycarbonate disk of a DVD-R followed by washing with ethanol. No further modification of the master mold was necessary. Similar work was also reported by Hong et al., where a nano-transfer mold was created using a SiO₂–TiO₂ sol–gel solution and the metal film from DVD and Blu-Ray (BR) molds (0.25:1).⁵⁷ In our work, we instead have utilized the higher-aspect-ratio polycarbonate disk of DVD-R media (0.5:1).

Mild NIL conditions (90 $^{\circ}\text{C}$ at 1.72 MPa for 30 s) were used to imprint the pattern lines of the polycarbonate master mold into the PHEMA thin film. AFM was utilized to examine the size and shape of the features through the various processes (Figure 2). The mold had the following original dimensions: height, 190 nm; line width, 500 nm; and periodicity, 809 nm, as reported in Table 1. The patterned PHEMA layer had dimensions of height, 179 nm; line width, 450 nm; and periodicity, 816 nm. The slight decrease in pattern height and line width of the replicated layer is due to shrinkage and solvent loss

(54) Li, X.; Song, L.; Vogt, B. D. *J. Phys. Chem. C* **2007**, 112(1), 53–60.
 (55) Li, X.; Vogt, B. D. *Chem. Mater.* **2008**, 20(9), 3229–3238.

(56) Cavallini, M.; Bergenti, I.; Milita, S.; Ruani, G.; Salitros, I.; Qu, Z.-R.; Chandrasekar, R.; Ruben, M. *Angew. Chem., Int. Ed.* **2008**, 47(45), 8596–8600.
 (57) Hong, L.-Y.; Lee, D.-H.; Kim, D.-P. *J. Phys. Chem. Solids* **2008**, 69 (5–6), 1436–1438.
 (58) Mukherjee, R.; Sharma, A.; Patil, G.; Faruqui, D.; Sarathi, P.; Pattader, G. *Bull. Mater. Sci.* **2008**, 31(3), 249–261.

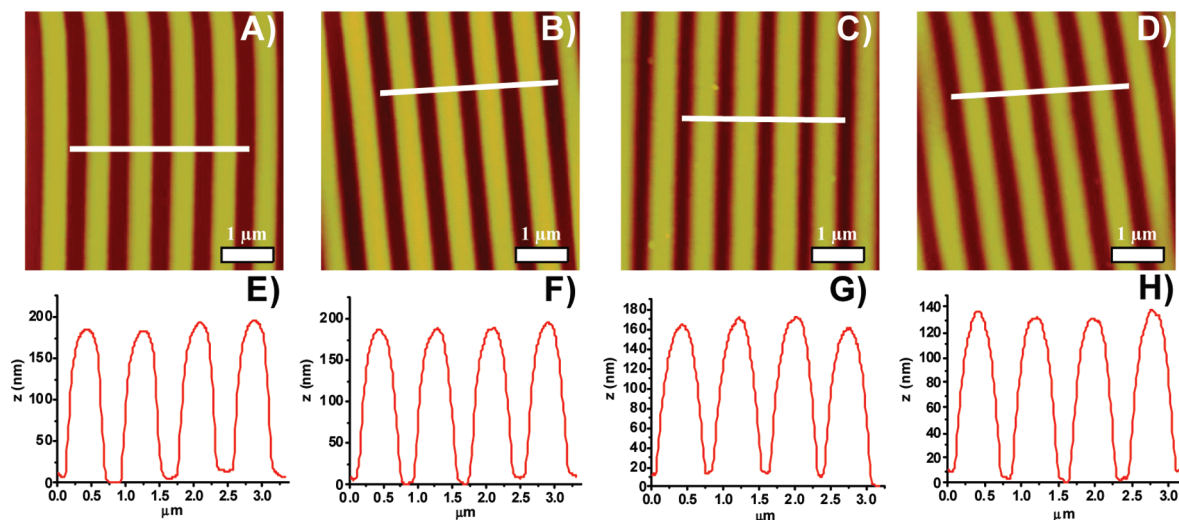


Figure 2. All AFM images reported are $5 \times 5 \mu\text{m}$ topographic images: (A) image of NIL patterned PHEMA 140 nm thin-film, (B) image of TCS cross-linked patterned PHEMA thin-film, (C) Image of scCO_2 TEOS infused thin-film, (D) image of calcined thin-film. (E–H) Tracer profile plots from the topographic images A–D, respectively.

Table 1. Summary of AFM Topographic Features Dimensions for Each Processing Step

sample	height (nm)	plateau width (nm)	periodicity (nm)
mold	187.5 ± 0.6	507.4 ± 8.5	808.8 ± 8.1
PHEMA patterned	179.0 ± 2.5	450.0 ± 2.9	816.5 ± 5.9
TCS (vapor) cross-linked	183.6 ± 3.9	484.4 ± 2.9	822.7 ± 4.1
scCO_2 infused	157 ± 3.7	481.8 ± 6.4	786.8 ± 11.1
calcined	129.5 ± 0.5	443.7 ± 4.9	759.1 ± 5.9
<hr/>			
	gap height (nm)	gap width (nm)	wall thickness (nm)
air-gap	65.2 ± 8.1	300.3 ± 12.1	70.8 ± 7.5

during the imprint process. Overall, the periodicity of the pattern remained constant and final dimensional control can be obtained by taking into account resin shrinkage during imprinting and solvent removal. Several AFM images were collected at arbitrary locations over the entire substrate, resulting in essentially identical images. Uniformity across the entire sample was observed, which implies that this process is likely limited only by the size of the master mold and the substrate available. We believe this process has potential for large-scale role-to-role production similarly reported recently with polyvinylalcohol thin films.⁵⁸

The patterned samples were then exposed to tetrachlorosilane (TCS) vapor for 12 h in a dry N_2 purged I-Chem jar (60 mL) with a Teflon seal. The extent of chemical modification of the samples was monitored by contact angle and grazing angle reflectance (GATR)-FTIR with identically prepared samples void of patterns. Each of the patterned samples was also analyzed by contact angle with identical results. The elevated temperatures needed for the complete SiO_2 infusion of the patterned substrates required a chemical cross-linking reaction because of the low T_g of PHEMA ($T_g = 73.5^\circ\text{C}$). The cross-linking afforded by reaction of PHEMA with TCS imparted structural rigidity for the subsequent scCO_2 mediated TEOS infusion at 160°C .

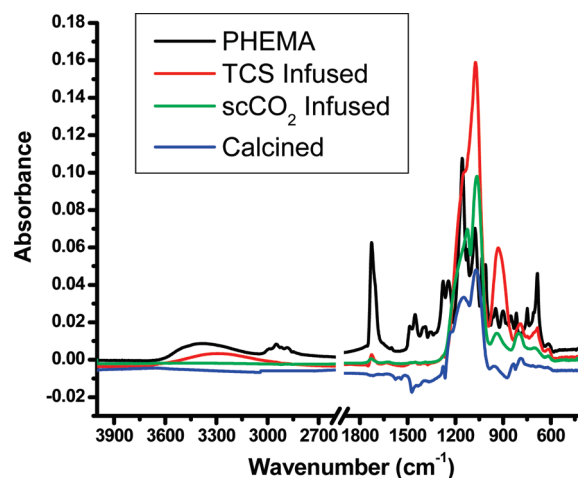


Figure 3. ATR-FTIR spectra of a PHEMA thin-film pretreated, exposed to TCS vapors for 12 h, scCO_2 infused with TEOS ($5 \mu\text{L}/\text{cm}^2$) for 12 h at 160°C , and calcined at 400°C for 6 h.

To ensure complete chemical cross-linking of the PHEMA substrate, we washed a test sample with methanol with no loss of pattern or observable change in the film thickness. Results in the ATR-FTIR spectra (Figure 3) confirmed a chemical change in the films during the various stages of processing with a decrease in the magnitude of the carbonyl vibrational stretch 1725 cm^{-1} $\nu(\text{C}=\text{O})$ and a dramatic increase in the peaks $1300\text{--}1000 \text{ cm}^{-1}$ characteristic of $\nu(\text{Si}-\text{O})$ and $\nu(\text{C}-\text{O})$ stretching vibrations. After the TCS chemical cross-linking, an intense peak appeared at 933 cm^{-1} , which corresponds to a silanol vibrational stretch $\nu(\text{Si}-\text{OH})$.⁵⁹ A characteristic broad peak $3600\text{--}3000 \text{ cm}^{-1}$ $\nu(\text{O}-\text{H})$ was evident in both the PHEMA and TCS cross-linked thin films, which represents a combination of the silanol and

(59) Pretsch, E.; Bühlmann, P.; Badertscher, M. *Structure Determination of Organic Compounds*, 4th ed.; Springer: Berlin, 2009; p 436–491.

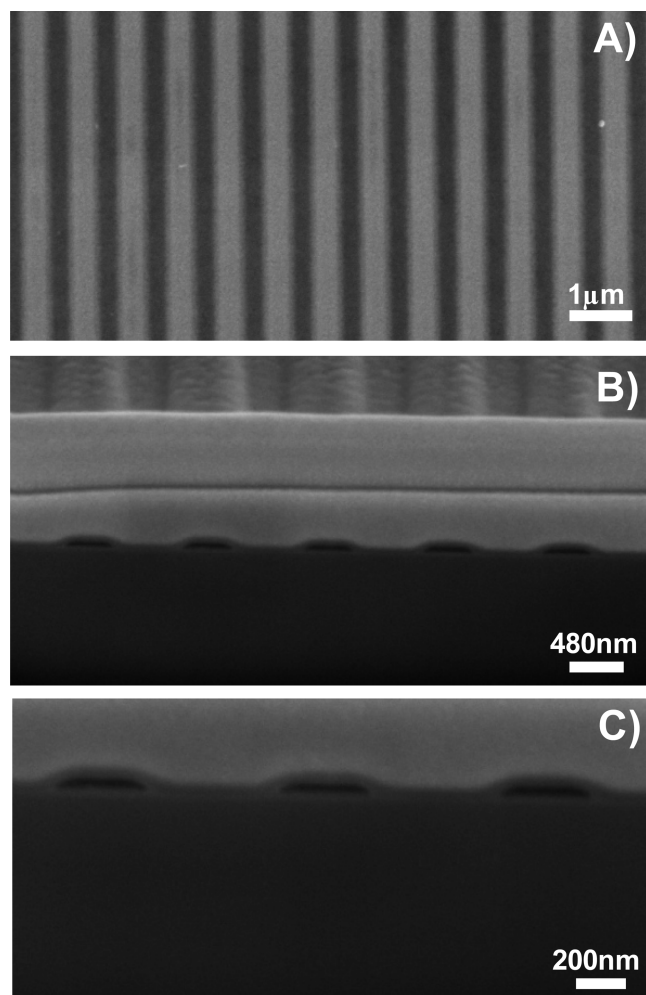


Figure 4. (A) SEM SiO_2 measured feature heights of ~ 130 nm, line width of ~ 450 nm, and a periodicity of ~ 760 nm over ($3.8 \text{ cm} \times 3.8 \text{ cm}$) substrate; (B) FIB SEM of SiO_2 air-gap patterns (calcined); large mound above patterned lines is deposited platinum; (C) FIB SEM (zoom) of SiO_2 air-gap patterns (calcined) center of image A. Height of air-gap ~ 65 nm, wall thickness ~ 70 nm, and width of air-gap ~ 300 nm.

hydroxyl group on PHEMA and infused TCS as well as ambient adsorbed water in the thin film. Furthermore, a slight increase in the width (~ 30 nm) and height (~ 5 nm) of the patterned lines was observed in the AFM images. This was a result of the chlorosilane swelling the PHEMA film. Condensation of the silanol functionality in the film was limited in the cross-linking step by performing the reactions at room temperature in order to allow only slight cross-linking and enable considerable infusion of TEOS in the scCO_2 processing stage. More rigorous conditions produced a thick silica coating covering the patterns and causing a loss of feature dimensions. The TCS vapor penetration depth was limited by the experimental conditions, which resulted in the formation of a SiO_2 -rich shell in the patterns. The SiO_2 shell limited the penetration of TEOS by scCO_2 which resulted in the formation of an air-gap structure after thermolysis.

The scCO_2 mediated infusion which resulted in the formation of a rigid SiO_2 patterned substrate was

performed with TEOS ($5 \mu\text{L}/\text{cm}^2$) and H_2O ($50 \mu\text{L}$) at 160°C for 12 h. Postinfusion, the water contact angle remained at 0° , indicating a strongly hydrophilic surface. Calcination was performed at 400°C for 6 h to increase the extent of condensation in the silica network and to remove any remaining organics, as reported in the literature.⁵³ Small changes in the intensity of the FTIR spectra were observed but no appearance/disappearance of any additional peaks as a result of the removal of the polymer template during calcination. A decrease in the height features by (~ 50 nm) was observed with an equivalent decrease in the line width (~ 440 nm) and periodicity (~ 760 nm). This decrease in the pattern dimension is a result of further condensation of the infused SiO_2 commonly reported in scCO_2 infusions a result of the dilatation of the polymer film with scCO_2 .⁵³ No change in the contact angle throughout the creation of these pattern SiO_2 lines was observed. The lines exhibited a uniform air-gap structure over the entire substrate with a height of (~ 65 nm), gap width (~ 300 nm), and wall width (~ 70 nm) was observed in the FIB SEM image reported in Figure 4. Uniform pattern lines over $10 \mu\text{m} \times 10 \mu\text{m}$ SEM scan reported in Figure 4A confirmed the AFM results. The cross-sectional SEM images shows pattern dimensions corresponding well with reported values determined by AFM. The percent shrinkage was $\sim 25\%$ for both the height and plateau width reported in Table 1 confirms the uniformity of this process with predictable processing dimensions. As a control experiment patterned PHEMA that had been reacted with TCS but not infused with TEOS was calcined under the same conditions (400°C soak for 6 h with a ramp rate of $1.67^\circ\text{C}/\text{min}$), which resulted in little to no pattern retention. A second control experiment in which the templates were exposed to TEOS vapor also failed to retain patterns, presumably because of limited diffusion rates of the precursor in the unplasticized templates.

Conclusions

The novel creation of air-gap SiO_2 features using NIL of polycarbonate molds into a functional polymer followed by scCO_2 infusion has been demonstrated. Virtually defect-free patterns with feature heights of ~ 130 nm, line widths of ~ 450 nm, and a periodicity of ~ 760 nm over large ($3.8 \text{ cm} \times 3.8 \text{ cm}$) substrates were generated after calcination. A uniform air-gap structure a result of vapor cross-linking was observed with a height of (~ 65 nm), gap width (~ 300 nm), and wall width (~ 70 nm). Structure evolution was followed by AFM, ATR-FTIR, and contact angle experiments that confirmed uniform pattern replication was performed as well as the complete chemical decomposition of the PHEMA polymer template at 160°C during the scCO_2 infusion and calcination steps. A wide range of applications requiring patterned oxide layers, including microfluidics, diffraction gratings, waveguides, and optical structures could be enabled by this new process. Other processes

that form SiO_2 patterns with sol–gel chemistry and acid-catalyzed solution infusion cannot be easily extrapolated to fabricate patterned free-standing structures and air-gap structures. Further modification of this process by exchanging the metal oxide precursor would allow the universal adaptation of this process to solar cells with metal oxides such as TiO_2 . This process is also adaptable to nanofluidics material separation through incorporation

of block copolymer templates, which will be discussed in subsequent publications.

Acknowledgment. This work was supported by the UMass Center for Hierarchical Manufacturing, a National Science Foundation Nanoscale Science and Engineering Center (NSEC) (CMMI-0531171). The S3IP Analytical and Diagnostics Laboratory at Binghamton University for FIB SEM images especially In-Tea Bae and Dae Young Jung.